

Theoretical characterization of SOME amides and esters DERIVATIVES of valproic acid

Nieves C. Comelli · Patricio Fuentealba ·
Eduardo A. Castro · Alicia H. Jubert

Received: 19 April 2009 / Accepted: 3 June 2009 / Published online: 16 July 2009
© Springer-Verlag 2009

Abstract The equilibrium structures, the planarity of the C (=O)X linkage and the nature of the chemical bond in the $Y-C(=O)-XR_1R_2$ [where: $Y = -CH-(CH_2-CH_2-CH_3)_2$, $X=N,O$ and $R_1, R_2 = H$; alkyl and aryl groups and lone pair electrons (lp)] molecular fragment of derivatives of Valproic acid (Vpa) with antiepileptic activity were studied systematically by means of B3LYP calculations and topological analysis of the electron localization function (ELF). The covariance parameter $cov[\Omega_i, \Omega_j]$ reveals a dominating delocalization effect between the lone pair $V(O_1)$, $V(X)$ and the electron density of the H–C and H– X_1 bonds resulting from the existence of not only non-conventional intramolecular hydrogen bonding patterns as C–H...O/N but also a weak closed-shell stabilizing interaction type arising from a dihydrogen bonding as C–H...H–N, where H...H contacts at a significantly shorter distance than twice the hydrogen atom van der Waals radius. The analyzed data derived from ELF domains were found to be in agreement with the known features and properties of the hydrogen bonding interactions discussed in this work.

N. C. Comelli · E. A. Castro
INIFTA, Theoretical Chemistry Division,
Suc. 4, C.C. 16, La Plata 1900,
Buenos Aires, Argentina

P. Fuentealba
Departamento de Física, Facultad de Ciencias,
Universidad de Chile,
Las Palmeras 3425, Ñuñoa,
653 Santiago, Chile

A. H. Jubert (✉)
Departamento de Química, Facultad de Ciencias Exactas, UNLP,
CEQUINOR, Centro de Química Inorgánica (CONICET, UNLP),
C. C. 962, 1900 La Plata. Facultad de Ingeniería, UNLP, 1 y 47,
1900 La Plata, Argentina
e-mail: jubert@quimica.unlp.edu.ar

Keywords Antiepileptic drugs · DFT · ELF ·
Electronic delocalization · Non-conventional hydrogen bonds

Introduction

The demand for new drugs for the treatment of epilepsy, which is one of the most common brain disorders, is still very high. Conventional antiepileptic drugs fail to control the occurrence of seizures at the extent of 30% [1]. Moreover, the use of these drugs is often precluded by the occurrence of untoward side-effects such as ataxia, diplopia, mental dulling, rash, blood dyscrasias, and hepatotoxicity.

Since the discovery of the anticonvulsants ability of valproic acid (Vpa), many similar compounds were studied in order to find new structures that are more powerful and possessing a lower neurotoxicity level.

Keane and Loscher [2, 3] had made modifications on length, saturation and branching of the aliphatic chains of Vpa, and they could propose a significant correlation between the length of the aliphatic chains and anticonvulsants power of Vpa derivatives. These authors noted that while the decrease in the length of the side chains cause the weakening or disappearance of the activity whereas the elongation of chains generated more active analogues with major sedative and hypnotic side effects. On the basis of these findings they have proposed that the Vpa presents the optimal chemical structure with regard to the limit between anticonvulsant activity and sedative and hypnotic side-effects.

With the discovery of considerable teratogenicity of Vpa in humans [4, 5], the search of new alternative structures was aimed to remove this toxic effect by taking care of keeping the effectiveness of antiepileptic drugs.

Nau and Loscher had reported on the synthesis and assessment of new compounds have been oriented on how functional changes in Vpa alter the manifestation of teratogenicity [6]. Comparative analysis of anticonvulsant potency and safety margin by utilizing the classical animal model for anticonvulsant screening had indicated that the functionalization of Vpa to amide provides greater anti-epileptic potential and lower teratogenicity due to the lack of the carboxyl group in these new molecules [6].

Later studies estimating the effectiveness and limitations of Valpromide (Vpd) to act as an antiepileptic drug (DAE) in humans concluded that its pharmacological selectivity is strongly conditioned by its biotransformation to Vpa. This fact shows that Vpd is a prodrug of Vpa when administered in humans [10]. Pharmacokinetic studies of various N-mono and N,N-disubstituted VPD derivatives seems to demonstrate that with the substitution in the amidic N, Vpd ceases to act as prodrug or a delayed release form of Vpa [7–11].

Another advantage observed with the substitution on the amide moiety is that the difference in Vpd derivatives which do not inhibit the microsomal epoxide hydrolase enzyme (mEH). The latter side effects the use of primary amides VPA has important toxicological implications since mEH is one of the most important enzyme in the detoxifying of reactive epoxide intermediates formed by oxidative metabolism of xenobiotics [7–11].

Recent results have been reported on the design, synthesis and biological evaluation in mice of some novel antiepileptic ligands derivatives of Vpd which are promising in establishing the new set of structures as promising candidates for the development of new drugs. These compounds comply with a pharmacophore model that establishes the essential structural and electronic features responsible for the protection against the maximal electroshock test (MES) [12, 13].

In an effort to determine the minimal structural requirement to produce anticonvulsant activity, Tasso *et al.* [12, 13] by using indirect methodologies for designing drugs and quantum chemical derived descriptors on bioactive conformations of *antiMES* drugs have reported that for a structure to elicit the anticonvulsant activity it is necessary the presence in their molecular architecture of an acceptor/donor unit comprising two closely located H-donor-acceptor groups and a lipophilic portion.

On the basis of this pattern, Tasso *et al.* [12, 13] have worked on the design, synthesis and biological evaluation of the derivatives of Vpa with a steric contour and degree of flexibility which could meet the structural and electrostatic requirements of the *antiMES* pharmacophore recently described by Gavernet *et al.* [14].

Tasso *et al.* [12, 13] have succeeded in characterizing the pharmacological profile of Vpd-related AEDs. Their argu-

ments are in the line with those reported for this region in [14].

Due to the absence of structural data in the literature on the drug-receptor complex during the anticonvulsant activity and assuming that the global minimum conformational defines the main properties of a compound, we are proposing here to explore and to characterize qualitatively and quantitatively the structural and electronic properties of the derivatives of Vpa in its ground state in order to arrive to a deeper understanding of the differentiated anticonvulsant behavior reported earlier [12, 13].

For this purpose we have performed a structural characterization by means of the topological analysis of the electron localization function (ELF) of Valpromide (Vpd), N-ethylvalpromide (Etvpd), dimethylvalpromide (Dmvpd), N-isopropylvalpromide (Ivpdp), propyl valproate (Prvp) and N-benzhydrylvalpromide (Bzvpd) (pharmacological behavior has not been determined since it is not soluble enough in the solvent (30% polyethylene glycol 400-PEG and 10 % water) employed to prepare the solution to administer intraperitoneally in mice) [12, 13]. We have also included in the present study the amides and esters whose synthesis and pharmacological behavior have not been reported up to now. These compounds are N-ethylaminevalpromide (Etavpd), N-Alphafenetylvalpromide (Aphvpd), isopentyl valproate (Ispvpa), Benzyl valproate (Benvpa) and 1-secbutanol valproate (Secbvpa). Although the anticonvulsant activity of this subset of amides and esters has been known we have included them in this study because they have an electrostatic and steric contour which match with the new requirement for the *antiMES* 3D pharmacophore as described in earlier [14].

We had used the results of topological analysis of the ELF to determine the nature of the electronic interaction within the C(=O).N and C(=O).O groups and how these groups are changed with respect to the kind of substituent linked to the amide and ester moieties.

Computational methodology

The conformational space of Vpa and derivatives are investigated using molecular dynamic simulations and the MM+ force field, both available in the HyperChem package [15]. The starting geometries have been generated heating from 0 to 900 K in 0.1 ps. Temperature was kept constant by coupling the system to a thermal bath with relaxation time of 0.5 ps. A 500 ps long simulation is performed after an equilibration period of 10 ps, saving molecular cartesian coordinates every 10 ps. The time step for the simulations is 0.1 fs. Outcome geometries were then optimized to an energy gradient less than $0.001 \text{ kcal mol}^{-1} \text{ \AA}^{-1}$ using the

semiempirical method AM1 as implemented in the HyperChem package [15].

A full geometry re-optimization of the lowest-energy conformers, obtained according to the above methodology, and vibrational analyses to characterize the minima were performed. We used the force gradient Bernys' algorithm method [16] and the density functional theory implemented in the Gaussian 03 package [17]. It comprises the Becke's three parameters hybrid functional [18], the Lee-Yang-Parr correlation functional [19] (B3LYP), including 6-31+G** as basis set.

Calculations of the electron localization function (ELF) were performed with the TOPMOD program package [20, 21] using wavefunctions obtained at the B3LYP/6311++G** level of theory from the Gaussian 03 suite. Visual rendering of synaptic basins was carried out using the outputs obtained from TopMod program and visualized with the Molekel package [22]. For the accuracy of the basin integration a threshold value of 10^{-7} has been adopted.

The topological analysis of the electron localization function (ELF) has been widely used as a convenient descriptor of chemical bond in various systems [23]. The description of the method has been given elsewhere [23–26] and will not be presented here.

We present an analysis of structural and electronic properties of valproic acid (Vpa), valpromide (Vpd), N-ethylvalpromide (Etvpd), dimethylvalpromide (Dmvpd), N-isopropylvalpromide (Ivpdp), N-ethylaminevalpromide (Etvpd), N-Alphafenetylvalpromide (Aphvpd), N-benzhydrylvalpromide (Bzvpd) and esters propyl valproate (Prvpa), isopentyl valproate (Ispvpa), Benzyl valproate (Bezvpa) and 1-secbutanol valproate (Secbvpa) by means of the analysis of the mean electron population N of core and valence basins, the population variance (σ^2), the relative fluctuation values and the covariance contributions to the electron density fluctuation calculated for ELF basins [24–26].

Results and discussion

The nomenclature and optimized molecular structures of the 12 selected compounds are depicted in Table 1 and Fig. 1, respectively. To the best of our knowledge, there is not in the standard literature information over X-ray diffraction data of Vpa, esters and N-mono and N,N-disubstituted derivatives of Vpa. Therefore, the report of theoretically calculated structural parameters may give suitable results about the geometry of $Y-C(=O)-XR_1R_2$ molecular fragment [where: $Y = -CH-(CH_2-CH_2-CH_3)_2$, $X = N, O$ and $R_1, R_2 = H$; alkyl and aryl groups and lone pair electrons (lp)] by aiming to know how it changes with

the type of substituents bonded to the amide and ester groups.

Equilibrium geometries

The distance and bond angles of the Vpd and Vpa derivatives obtained at the B3LYP/6311++G** level of theory are listed in Table 2 and 3, respectively. These theoretical data compared with the distances and the angles among the core attractors derivated from ELF topologies in order to evaluate the possibility of using the later as indicators of the most probable position of an electron pair in the sense of the Gillespie model [27]

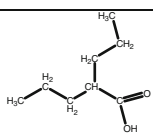
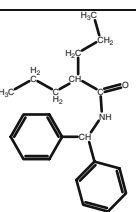
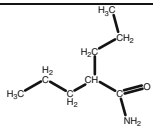
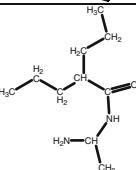
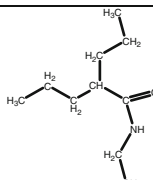
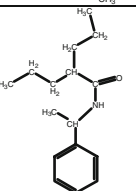
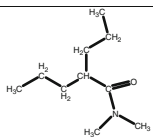
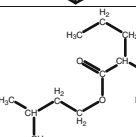
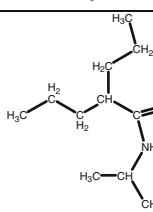
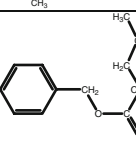
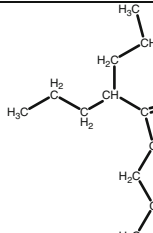
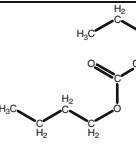
The root mean square (RMS) was determined from the difference between the geometrical parameters of Etavpd, Aphvpd, Bzvpd, Etvpd, Dmvpd, Vpd, Ivpdp, Prvpa, Ispvpa, Secbvpa, Bezvpa, and Vpa in the gas phase. The position of the respective attractors was found as ~ 0.032 Å by considering the bonds lengths, while the corresponding difference for bond angles is $\sim 2.5^\circ$. These results show that the position of the attractors correlate quite well with the nuclei positions. Moreover, it can be concluded that the stereochemistry information derived from *ab-initio* calculations on the basis of molecular symmetry arguments is limited, so any analysis derived from the use of structural parameters obtained from ELF calculations can be helpful.

The optimized geometries of aliphatic portions in the studied compounds suggested that this region is strictly formed by carbon-carbon and carbon-hydrogen single bonds as the C–C and C–H bonds lengths lying in the range of 1.535–1.537 Å and 1.094–1.097 Å and the bond angles C–C–C, C–C–H, and H–C–H values fall within the range 111.8–113.1°, 109.4–109.6°, and 106.9–107.2, respectively (Table 2 and 3). The bonds in CH_2 and CH_3 moieties are arranged in staggered conformations (there are found no eclipsed bonds) (Fig. 1).

For the structural parameters that describe aromatic substituent binding to $-C(=O)-N-$ and $-C(=O).O-$ groups, the calculated bond lengths and bond angles are in very good agreement with the stereochemical feature of planar conjugated systems involving carbon atoms with a trigonal geometry (Tables 2 and 3).

With respect to the calculated bond lengths and bond angles in $-C(=O)-X$ polar fragments, they are in quite satisfactory agreement with the peculiar geometries of amide and esters in a way that bond lengths and angles are consistent with a sp^2 hybridization for the C, N, and O atoms [28]. The differences in the bond distances observed along the set of derivatives of the Vpa [0.022 Å for C–N, 0.007 Å for C–O and 0.035 Å for C=O] (Tables 2 and 3) can be correlated *a priori* on the basis of a non uniform resonant effect within the $C(=O)-X$ moiety. These changes

Table 1 Nomenclature and molecular formula of the 12 selected compounds

Nomenclature in the text	IUPAC nomenclature	Molecular Formula	Nomenclature in the text	IUPAC nomenclature	Molecular Formula
Valproic acid	2-propylpentanoic acid		N-benzhydrylvalpromide	<i>N</i> -(1,1-diphenyl)methyl-2-propylpentanamide	
Valpromide	2-propylpentanamide		<i>N</i> -ethylaminevalpromide	<i>N</i> -(2-amino)ethyl-2-propylpentanamide	
<i>N</i> -ethylvalpromide	<i>N</i> -ethyl-2-propylpentanamide		<i>N</i> -Alphafenetylvalpromide	<i>N</i> -(1-phenylethyl)-2-propylpentanamide	
dimethylvalpromide	<i>N,N</i> -dimethyl-2-propylpentanamide		isopentyl valproate	Isopentyl 2-propylpentanoate	
<i>N</i> -isopropylvalpromide	<i>N</i> -isopropyl-2-propylpentanamide		Benzyl valproate	benzyl 2-propylpentanoate	
propyl valproate	propyl 2-propylpentanoate		1-secbutanol valproate	(1-methyl)propyl 2-propylpentanoate	

were investigated in detail from the analysis of the ELF calculations.

With regard to 3D arrangements of the atoms in the polar regions of these molecules, the most remarkable geometrical feature is that the amide and ester linkage have an antiperiplanar (*anti*) configuration (*i.e.*, dihedral angle close to 180° for the C_α – C(=O) – X – C axis). The positions adopted by the substitutions at the acyl moiety have very weak steric interaction with the other portion of the molecule in a way that the side chains linked to acyl moiety (*N*-acyl) are placed parallel to propylic chains by gaining conformations *syn* to the C=O bond. The preference for this orientation may be mainly attributable to the

minimization of the electronic repulsion between the different substituents (acyl group, H, alkyl and aryl groups and the oxygen lone pairs) around the amide and ester functionality (Fig. 2).

Regarding the planarity of C(=O)–X, the out-of plane deformations are characterized by the calculation of Winkler-Dunitz parameters [29], which represent the twisting around the C–X bond (τ) and the pyramidal out-of-plane deviations on the carbonyl carbon and nitrogen atoms (χ_C , χ_X = bonds-to-carbon and bonds-to-X out-of-plane deviation). Internal coordinate set describing the deformation of Y–C(=O)–XR₁R₂ fragment are shown in Fig. 3.

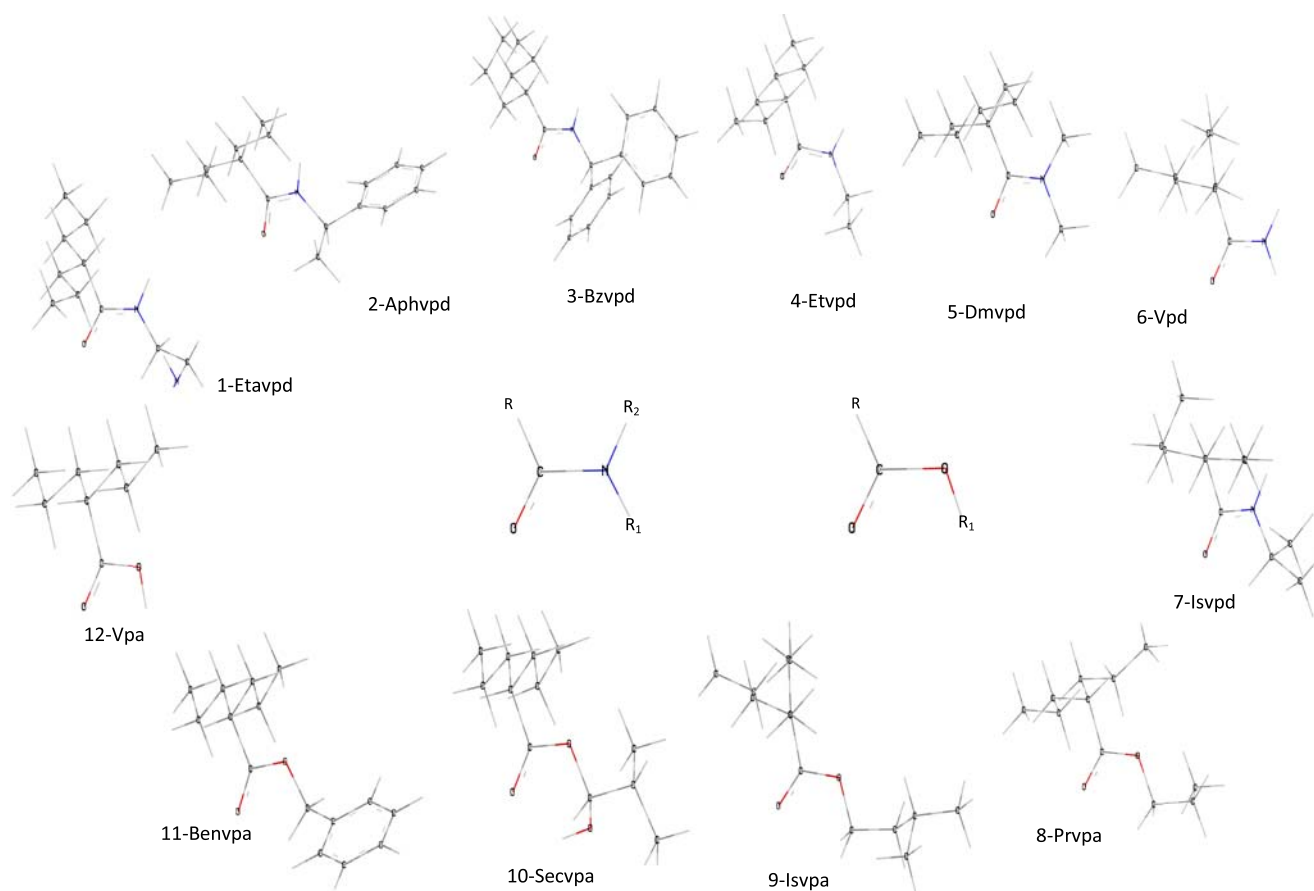


Fig. 1 Amide and esters set optimized at the B3LYP/6-31+G** level of theory. Three different molecular structure for this molecules were characterized depending on the group attached to the amidic nitrogen

($R_1 = \text{H}, -\text{CH}_3, -\text{CH}_2-\text{CH}_3, -\text{CH}_2-\text{CH}_2-\text{NH}_2, -\text{CH}(\text{CH}_3)_2, -\text{CH}(\text{CH}_3)(\text{C}_6\text{H}_5)$ and $-\text{CH}(\text{C}_6\text{H}_5)_2$; and from $R_2 = -\text{H}, -\text{CH}_3$ or lp). In this figure $R = -\text{CH}-(\text{C}_3\text{H}_7)_2$

Tables 2 and 3 list the value of the descriptors of out-of-plane deformations (τ, χ_C, χ_X) calculated from the cartesian coordinates of the attractor position of the $\text{C}(\text{=O})-\text{X}$ backbone described with the procedure [29].

The data indicate that the planarity of $\text{O}=\text{C}-\text{X}$ backbone are moderately influenced by the type, number, and size of substituents. In general it is observed that the twisting around the $\text{C}-\text{X}$ bond increases as we move from 1 to 12 (Fig. 1, Tables 2 and 3). Compared with the geometry of primary and secondary amides of Vpa (Table 2), the esters present larger twisting angles τ , the bonds-to-carbon out-of-plane deformation (χ_C) is smaller since the observed distortions do not exceed 2.5° and the pyramidalization on the ester oxygen (χ_O) which is strongly coupled to the τ angle, is slightly larger than χ_N (Table 3).

The slightly larger pyramidalization of the X atom regarding the description of the carbonyl carbon shows clearly the moderating role of substituents linked to acyl moiety on the conformations of $\text{C}(\text{=O})\text{X}$ skeleton. In fact, our results indicate that the $\text{C}-\text{X}$ bond is slightly elongated and the $\text{C}=\text{O}$ bond is shortened with the variation of τ (Tables 2–3). Regarding to the pattern of change of $\text{C}-\text{X}$

and $\text{X}-\text{C}$ bond lengths it can be seen that the variations of bond lengths are most significant in amides than esters and Vpa, and that these changes increase with the increasing of the steric bulkiness of the N-acyl group [$R_1 = \text{aryl}$] (Tables 2–3).

In order to examine the decreasing effect of the steric strain around the $\text{C}-\text{X}$ bond the distances between the neighboring $\text{C}-\text{H}$ at the atoms in the $\text{C}(\text{=O})-\text{X}$ backbone (*i.e.*, $\text{C}-\text{H}\dots\text{O}$ and $\text{C}-\text{H}\dots\text{N}$) (Fig. 4) have been evaluated. Surprisingly, the mean interatomic distances turned out to be shorter than the conventional sum of the van der Waals radii ($d_{\text{H}\dots\text{O}}, d_{\text{H}\dots\text{N}} < \sum r(\text{vdW})[\text{H}, \text{O}][\text{H}, \text{N}] \sim 2.75 \text{ \AA}$) and regarding to the value of $d_{\text{H}\dots\text{O}}, d_{\text{H}\dots\text{X}}$, they depend on the nature of the H atom: the shorter distances are centered around 2.5 \AA and these values change with the decreasing of acidity of the $\text{C}-\text{H}$ bond [$d_{\text{C}(\text{sp})-\text{H}\dots\text{O}, \text{X}}^2 < d_{\text{C}(\text{sp})-\text{H}\dots\text{O}, \text{X}}^3$].

These results reveal that, for a given combination of out-of-plane bending distortion, the conformation in the $\text{O}=\text{C}-\text{X}$ moiety, seems to be not only regulated by the sterical effects between R, R_1 and R_2 but also by the formation of intramolecular hydrogen bonding. In fact, the structural change induced to the atoms in $\text{O}=\text{C}-\text{X}$ lean away from co

Table 2 Structural data and Winkler-Dunitz parameters of N-ethylaminevalpromide (Etavpd), Alphafenetylvalpromide (Aphvdp), N-benzhydrylvalpromide (Bzvdp), N-ethylvalpromide (EtVpd), dimethylvalpromide (Dmvpd), valpromide (Vpd) and N-isopropylvalpromide (Ivpd)

	Parameters	Etavpd	Aphvdp	Bzvdp	EtVpd	Dmvpd	Vpd	Ivpd
alkyl groups	C-C	1.537(1.534)	1.533(1.534)	1.536(1.533)	1.536(1.533)	1.536(1.540)	1.537(1.535)	1.536 (1.542)
	(C-C)r*	1.541 (1.538)	1.529 (1.539)	1.528 (1.531)	1.531(1.533)	-	-	1.532 (1.531)
	C-H	1.097 (1.121)	1.124 (1.121)	1.097 (1.120)	1.097 (1.121)	1.097 (1.121)	1.097 (1.120)	1.096 (1.120)
	(C-H)r	1.098 (1.123)	1.094 (1.118)	1.095 (1.115)	1.094 (1.120)	1.094 (1.119)	-	1.094 (1.119)
	C-C-C	112.7 (113.5)	112.2 (112.4)	113.1 (111.9)	112.1 (112.5)	111.9 (112.5)	112.2 (112.5)	112.9 (113.1)
	(C-C-C)r		113.7 (112.3)	114.2 (112.1)			-	112.4 (111.8)
	C-C-H	109.5 (109.3)	109.5 (109.7)	109.5 (110.7)	109.6 (108.6)	109.6 (109.3)	109.6 (109.1)	109.5 (109.7)
	(C-C-H)r	109.3 (110.7)	109.5 (110.7)	107.9 (107.6)	110.6 (111.1)		-	109.9 (107.7)
	H-C-H	107.3 (107.7)	107.2 (108.7)	106.9 (107.6)	107.2 (106.4)	107.2 (106.8)	107.2 (107.7)	107.1 (110.7)
	(H-C-H)r	107.2 (107.9)	108.5 (107.6)	-	108.1 (107.9)	108.9 (108.5)	-	108.1 (108.1)
Aryl group	C=C	-	1.399 (1.402)	1.397 (1.394)	-	-	-	-
	(C-H)a		1.086 (1.109)	1.086 (1.108)	-	-	-	-
	N-C-C=	-	-	111.2 (111.6)	-	-	-	-
	C-C=C		120.1 (120.6)	120.7 (121.5)	-	-	-	-
	H-C=C	-	119.9 (118.8)	120.1 (119.6)	-	-	-	-
Polar group	C=O	1.246 (1.246)	1.232 (1.232)	1.227(1.228)	1.231(1.231)	1.247 (1.247)	1.227(1.227)	1.228 (1.229)
	C-N	1.353 (1.354)	1.365 (1.365)	1.371 (1.374)	1.367 (1.367)	1.364 (1.365)	1.368 (1.369)	1.366 (1.367)
	N-C	1.459 (1.460)	1.473 (1.473)	1.465 (1.465)	1.460 (1.460)	1.462 (1.462)	-	1.465 (1.466)
	N-H	1.023 (1.044)	1.0098 (1.031)	1.010 (1.032)	1.0095 (1.031)	-	1.010 (1.028)	1.0097 (1.031)
	C-C=O	121.3 (123.7)	124.7 (124.1)	122.1 (124.3)	121.6 (124.2)	118.3 (116.6)	122.4 (124.8)	121.5 (124.2)
	C-C-N	116.1 (116.4)	116.275 (116.1)	115.6 (115.6)	116.1 (119.9)	120.9 (120.2)	116.0 (114.8)	116.1 (115.8)
	O=C-N	122.5 (119.8)	121.9 (119.7)	122.3 (119.9)	122.3 (119.9)	120.7 (123.2)	121.6(120.4)	122.3 (119.5)
	C-N-H	118.0 (119.4)	118.6 (120.1)	118.1 (116.4)	118.1 (119.4)	-	120.5 (122.4)	118.6 (117.7)
	H-N-H	-	-	-	-	-	118.5 (118.6)	-
	N-(C-C)r	116.4 (117.4)	111.3 (109.4)	111.2 (110.6)	113.2 (110.9)		-	110.5 (109.7)
	(C-N)r	1.370 (1.354)						
	(N-H)r	1.01 (1.043)	-	-	-	-	-	-
	(H-N-H)r	106.6 (106.7)	-	-	-	-	-	-
(N-C-H)r	108.2 (108.8)	-	103.7 (104.8)	109.3 (108.9)	110.4 (110.1)	-	-	
Planarity	τ	0.150	0.176	0.231	0.501	0.715	1.002	1.206
	χ_C	1.201	4.749	13.89	3.138	2.483	1.012	7.204
	χ_N	4.138	1.640	4.780	0.880	1.041	1.184	2.053

*r = Structural data corresponding to geometry of alkyl substituent linked to polar group

planarity is accompanied by a proper three-dimensional arrangement of the proton donor and the proton acceptor units in the structure under study that leads to the formation of non-classical intramolecular bonds (Fig. 4).

ELF analysis

The ELF topology of the aliphatic portions in the Y-C(=O)-NR₁R₂ and Y-C(=O)-OR₁R₂ molecules is of the same type in all investigated structures. These topologies consist of core attractors associated with core electron densities of the carbon atoms C(C), disynaptic valence

attractors V(C,C) located between the core which describe the C-C bonds and protonated disynaptic valence attractors V(H,C) surrounding each core describing the C-H bonds (Fig. 5). The number of V(C,C) and V(H,C) bonding basins matches with the coordination number of each atom (electronic octet) in R, R₁ and R₂ and they are arranged according to the prescriptions of Gillespie-Nyholm rules [29].

The ELF topology of the aryl groups (Fig. 5), in each hexagonal conjugated structure C₆H₅- there exists only one disynaptic basin $v(C_{sp}^2, C_{sp}^2)$ between two successive carbons and five $v(H, C_{sp}^2)$ basins describing the C-H bonds.

Table 3 Structural data and Winkler-Dunitz parameters of propyl valproate (Prvpa), isopentyl valproate (Ispvpa), 1-secbutanol valproate (Sebvpa), benzyl valproate (Bezvpa) and valproic acid (Vpa)

	Parameters	Prvpa	Ispvpa	Sebvpa	Bevpa	Vpa
Alkyl groups	C-C	1.535(1.536)	1.535(1.536)	1.535(1.536)	1.537(1.537)	1.534(1.532)
	(C-C) _r *	1.526 (1.534)	1.533 (1.537)	1.5309 (1.532)	1.5309 (1.532)	
	C-H	1.095 (1.096)	1.096 (1.097)	1.097 (1.098)	1.097 (1.098)	1.097 (1.120)
	(C-H) _r	1.097 (1.098)	1.097 (1.096)	1.097 (1.098)	1.097 (1.098)	
	C-C-C	112.2 (112.1)	112.4 (112.4)	112.240 (112.1)	112.2 (112.1)	112.703 (112.3)
	(C-C-C) _r		112.8 (112.9)			
	C-C-H	109.5 (109.6)	109.7 (109.7)	109.5 (109.6)	109.5 (109.6)	109.7 (109.4)
	(C-C-H) _r	110.6 (110.6)	109.9 (109.9)	110.6 (110.6)	110.6 (110.6)	
	H-C-H	107.2 (107.7)	107.4 (107.6)	107.2 (107.7)	107.2 (107.7)	105.9 (106.0)
	(H-C-H) _r	107.4 (107.6)	107.4(107.6)	107.375 (107.6)	107.4 (107.6)	
Arylgroup	C=C				1.395 (1.394)	
	(C-H) _a				1.085 (1.108)	
	H-C=C	-	119.9 (118.8)	120.1 (119.6)	-	-
	O-C-C=				111.8 (111.9)	
Polar group	C=O	1.214 (1.224)	1.214 (1.224)	1.220 (1.224)	1.214 (1.224)	1.212 (1.212)
	C-O	1.353 (1.345)	1.353 (1.344)	1.348 (1.345)	1.356 (1.345)	1.360 (1.361)
	O-C	1.448 (1.457)	1.447 (1.458)	1.468 (1.457)	1.456 (1.457)	
	O-H					0.972(0.995)
	C-C=O	125.5 (124.8)	125.3 (124.6)	125.5 (124.8)	123.5 (124.9)	125.9 (128.9)
	C-C-O	111.2 (112.3)	111.4 (112.4)	111.2 (112.3)	111.2 (112.3)	112.2 (111.9)
	O=C-O	123.3 (122.8)	123.2 (122.9)	123.2 (122.8)	122.2 (124.8)	121.8 (119.2)
	C-O-C	116.0 (117.5)	115.9 (117.4)	116.0 (117.5)	116.02 (117.6)	
	O-C-C	107.9 (107.6)	108.0 (108.2)	108.2 (108.3)	108.0 (108.5)	
	O-C-H	108.7 (108.2)	108.7 (108.985)	108.1(108.5)	108.0 (108.2)	
Planarity	C-O-H					105.7 (103.9)
	τ	0.420	0.604	1.197	1.930	4.020
	χ_C	0.977	2.498	1.163	0.071	0.005
	χ_O	0.322	2.154	3.850	4.671	8.040

*_r = Structural data corresponding to geometry of alkyl substituent linked to polar group

The ELF topology of the O=C–X group was found to be the same type in all investigated structures. It consists of three core attractors associated with core densities of oxygen C(O₁), carbon C(C), and nitrogen C(N₁) (in amides) (Fig. 5c) or C(O₁), carbon C(C), and C(O₂) (in esters) (Fig. 5d); two monosynaptic valence attractors of oxygen V₁(O₁), V₂(O₁); two attractors V₁(N₁), V₂(N₁), one V₁(O₂) attractors and two valence disynaptic attractors V(C, O) and V(C, X=N, O), which describe the C=O and C–N/C–O bonds. The V₁(O₁), V₂(O₁), V₁(N₁), V₂(N₁), and V₁(O₂) basins represents the electron lone pairs of O and N which are oriented orthogonal to each other in the plane containing the C(=O)–X group (Fig. 5).

The description of the carbon-chalcogen bond which is formally a double bond depends on the basis set adopted for the computations [30].

Our calculations performed with the B3LYP/6–311++G (d,p) basis set yields only one V(C, O) basin in the

description of C=O bond and the partial π character of C–X is demonstrated from the fact that the V₁(N₁), V₂(N₁) and V₁(O₂) basins are not well resolved from the V(C, X) basins (Fig. 5).

The basin populations (\bar{N}), their variance and relative fluctuations computed for the (Pr)₂HC(=O)–NR₁R₂ and (Pr)₂HC(=O)–OR₁R₂ are collected in Tables 4 and 5, respectively. They are arranged following the increasing value of the τ dihedral angle (planarity deviation).

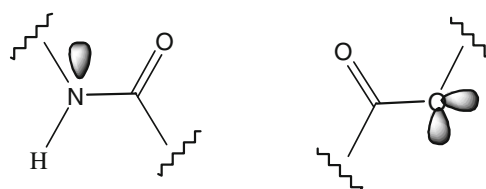


Fig. 2 Representation schematic of geometries around the amide and esters moieties

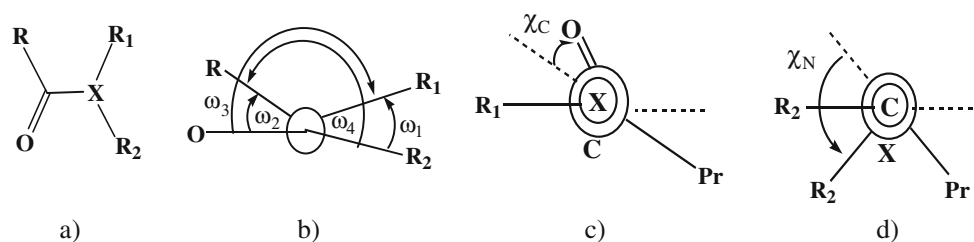


Fig. 3 In (a) $X=N,O$; $R=-CH-(C_3H_7)_2$; $R_1=H$; $-CH_3$; $-CH_2-CH_3$; $-CH_2-CH_2-NH_2$; $-CH(CH_3)_2$; $-CH(CH_3)(C_6H_5)$ and $-CH(C_6H_5)_2$; and from $R_2 = -H$, $-CH_3$ ó lp O. (b) The four dihedral angles used for determining the torsional angle τ and the pyramidity descriptors

χ_C . χ_X . (c) The angle χ_C and χ_X are defined as $\chi_C = \omega_1 - \omega_3 + \pi(\text{mod}2\pi) = -\omega_2 + \omega_4 + \pi(\text{mod}2\pi)$ and $\chi_X = \omega_2 - \omega_3 + \pi(\text{mod}2\pi) = -\omega_1 + \omega_4 + \pi(\text{mod}2\pi)$. The torsional angle τ is defined as $\tau = (\omega_1 + \omega_2)/2$

The mean electron population \bar{N} of the core basins localized both in R, R_1 and R_2 as well as in $C(=O)-X$ group, is calculated to lie between $2.09e$ for C, $2.10e$ for N and $2.12e$ for O and it is almost independent of the hybridization of the atoms (in propylic chains \bar{N}_{Csp^3} is equal to \bar{N}_{Csp^2} in amide and ester moieties). The variances and relative fluctuation range of the core basins C, N, and O populations is comprised between 0.26–0.34 and 0.13–0.16 respectively. We can notice that \bar{N} , σ^2 and λ enhance with the atomic number (Z) and it can be interpreted in terms of the variation of effective potential that feel the

valence electrons due to the increasing of the charge core (Table 4 and 5). Thus, it seems that the valence electrons of O and N atoms (nucleus with a minor core radius and major nuclear charge) are induced to enter in the core zone with more facility than in that one corresponding to the C atom.

On the basis of an interpretation given by Silvi and Savin [24–26], the populations of the $V(H,C)$ and $V(C,C)$ basins in the hydrophobic regions of different derivatives of Vpa show a clear covalent character with ranges between $2.0(C_{sp}^3 - H) - 2.15e(C_{sp}^2 - H)$ and $1.86(C_{sp}^3 - C_{sp}^3) - 2.14e(C_{sp}^2 - C_{sp}^2)$. The difference in value within each type of

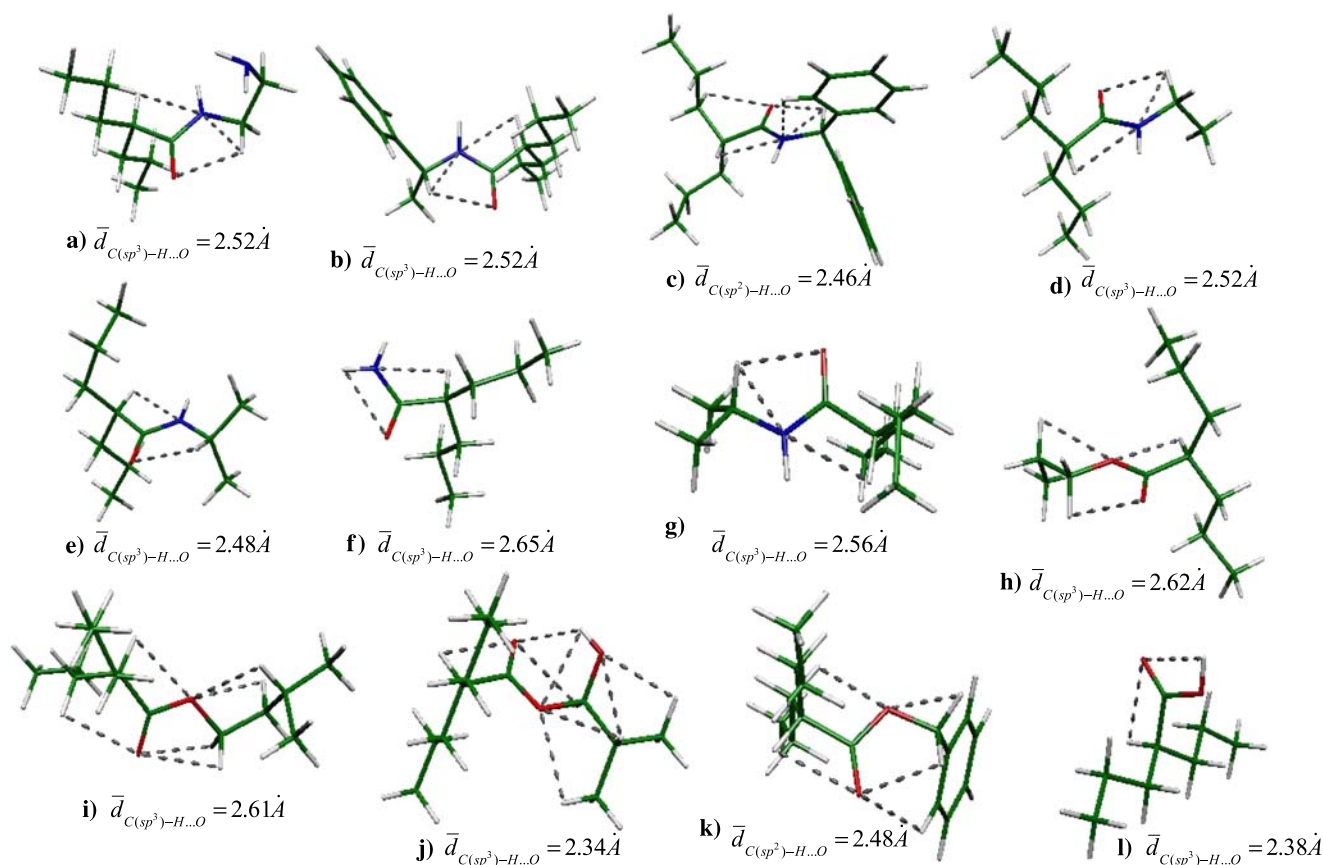


Fig. 4 Non-bonded distances between the C-H group neighboring at the atoms in the $C(=O)-X$ backbone in, (a) Etavpd, (b) Aphvpd, (c) Bzvpd, (d) Etvpd, (e) Dmvpd, (f) Vpd, (g) Ipvpd, (h) Prvpa, (i) Isovpa, (j) Secvpa, (k) Benvpa, and (l) Vpa

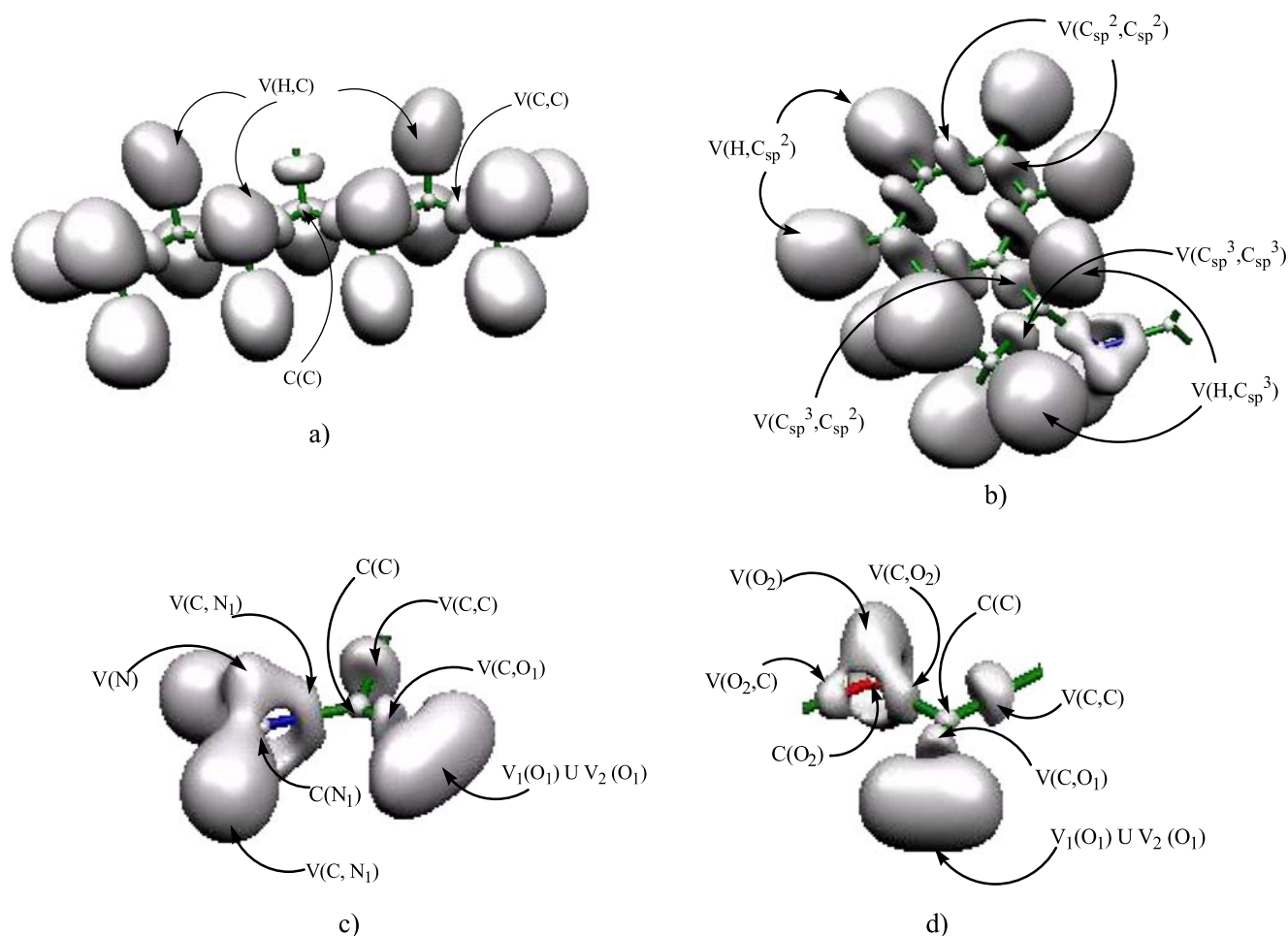


Fig. 5 3D plot of electron localization function (ELF) at $\eta(r)=0.80$ in: (a) propyl chains (b) aryl rest; (c) O=C-N group and (d) O=C-O group

basins [larger saturation of $V(H,C)$ and $V(C,C)$] can be justified in terms of the increase of electronegativity and bond order going from $C_{sp}^3 - C_{sp}^3$, $C_{sp}^3 - C_{sp}^2$ and $C_{sp}^2 - C_{sp}^2$ bonds. The high values of σ^2 and λ for these basins [0.66–0.99 and 0.33–0.53] in relation to those calculated for core basins suggest that in this molecular region the atoms are sharing an electron each other while forming bonds.

For the bonds in the $C(=O)-N$ planar region, the electron localization function analysis specify an interesting picture for valence shells as follows; the electronic population intermediate between that of a simple and a double bond for $C=O$ and $C-N$ [2.14–2.27 e in $V(C,O_1)$ and 2.96–2.13 e in $V(C,N_1)$ basins and bond order ~ 1.07 – 1.13 against ~ 1.48 – 1.06] with an important reorganization of the electron density within the amide group moving from Etavpd to Ippvdp (Table 4). The $V(H,N)$ basins have a population of almost $2e$ suggesting a simple covalent bond. With respect to the basins describing the lone electron pair of O and N [$V_{1,2}(O_1)$, $V_{1,2}(N_1)$], it is worth mentioning that due to the asymmetry of the molecules (point group of symmetry C_1) the electron lone pairs of O and N are not identical. An

analysis on the population of $V_{1,2}(O_1)$ and $V_{1,2}(N_1)$ basins (Table 4) reveals for $V_1(O_1) \cup V_2(O_1)$ domain an electron density being in the range from 5.54 e (Etavpd) to 5.44 e (Vpd) and for the $V_1(N_1) \cup V_2(N_1)$ domain the electron population is found to increase in the range of 1.04–1.99. The electronic reorganization observed in these domains can be rationalized in principle, in terms of the electronic distribution that minimize the Pauli repulsion of these basins with the adjacent [$V(H,C)$ and $V(C,C)$] ones.

Examining the basin populations on carboxylate moiety in Vpa and esters (Table 5) and comparing with the values for amides, our results reveal that these compounds present a larger $V(C,O_1)$ population ($\sim 2.4e$) and significantly smaller mean $V(C,O_2)$ population ($\sim 1.7e$) than its analogues in amides. Furthermore, the O_1 oxygen's lone pairs bear a smaller population than its analogues in amides and the basin populations of $V_{1,2}(O_2)$ and $V_{1,2}(O_3)$ basins found to have considerably less electrons than its analogue $V_{1,2}(O_1)$. An exception to this trend is found in the Secvpa, which display a large electron density on the lone pairs in the O_2 and that could be pointed out a noticeably electronic

Table 4 Basin populations (\bar{N}), the population variance $\sigma^2(\bar{N})$ and relative fluctuation λ in the N-ethylaminevalpromide (Etavpd), Alpha-fenetylvalpromide (Aphvdp), N-benzhydrylvalpromide (Bzvdp), N-ethylvalpromide (Etvpd), dimethylvalpromide (Dmvpd), Valpromide

(Vpd) and N-isopropylvalpromide (Ivpdp), propyl valproate (Prvpa), isopentyl valproate (Ispvpa), 1-secbutanol valproate (Secbvpa), benzyl valproate (Bezvpa), and valproic acid (Vpa)

Basins. Ω	Etavpd	Aphvdp	Bzvdp	Etvpd	Dmvpd	Vpd	Ivpdp
Properties $R=(Pr)_2 = -CH_2 CH_2-CH_3$							
	$N_\Omega(\sigma^2; \lambda)$	$N_\Omega(\sigma^2; \lambda)$	$N_\Omega(\sigma^2; \lambda)$	$N_\Omega(\sigma^2; \lambda)$	$N_\Omega(\sigma^2; \lambda)$	$N_\Omega(\sigma^2; \lambda)$	$N_\Omega(\sigma^2; \lambda)$
C(C)	2.09(0.26;0.13)	2.09(0.27;0.13)	2.09(0.27;0.13)	2.09(0.26;0.13)	2.09(0.26;0.13)	2.09(0.26;0.13)	2.09(0.26;0.13)
V(C,C)	1.86(0.99;0.53)	1.86(0.99;0.53)	1.87(0.99;0.53)	1.86(0.99;0.53)	1.90(1.0;0.53)	1.86(0.99;0.53)	1.86(0.99;0.53)
V(H,C)	2.01(0.66;0.33)	2.0(0.66;0.33)	2.01(0.66;0.33)	2.01(0.66;0.33)	2.0(0.66;0.33)	2.01(0.66;0.33)	2.01(0.66;0.33)
Properties $R_1=R_2=$ alkyl							
C(C)	2.09(0.26;0.13)	2.09(0.27;0.13)	2.1(0.26;0.12)	2.09(0.26;0.13)	2.08(0.26;0.13)	-	2.09(0.26;0.13)
V(C,C)	1.93(1.0;0.52)	1.91(1.0;0.52)	-	1.86(0.99;0.53)	-	-	1.9(0.99;0.52)
V(H,C)	2.04(0.66;0.32)	2.0(0.66;0.33)	2.01(0.67;0.33)	2.01(0.65;0.32)	2.02(0.65;0.32)	-	2.0(0.66;0.33)
C(N ₂)	2.1 (0.3;0.14)	-	-	-	-	-	-
V(N ₂ ,C)	1.67(0.96;0.57)	-	-	-	-	-	-
V(H,N ₂)	1.98(0.78;0.4)	-	-	-	-	-	-
V(N ₂)	2.14(0.98;0.46)	-	-	-	-	-	-
Properties $R_1=$ aryl							
C(C)	-	2.09(0.27;0.13)	2.1(0.26;0.12)	-	-	-	-
V(C _{sp} ³ , C _{sp} ³)	-	-	2.05(1.04;0.50)	-	-	-	-
V(C _{sp} ³ , C _{sp} ²)	-	2.05(1.03;0.50)	2.05(1.04;0.50)	-	-	-	-
V(C _{sp} ² , C _{sp} ²)	-	2.77(1.31;0.47)	2.77(1.31;0.47)	-	-	-	-
V(H, C _{sp} ³)	-	2.15(0.67;0.31)	2.0(0.67;0.34)	-	-	-	-
V(H, C _{sp} ²)	-	2.15(0.67;0.31)	2.15(0.67;0.31)	-	-	-	-
Properties C(=O)-N							
C(C)	2.09(0.26;0.12)	2.09(0.26;0.12)	2.09(0.26;0.12)	2.09(0.26;0.12)	2.08(0.26;0.12)	2.09(0.26;0.12)	2.09(0.26;0.12)
C(O ₁)	2.11(0.34;0.16)	2.11(0.35;0.17)	2.10(0.34;0.16)	2.1(0.34;0.16)	2.12(0.34;0.16)	2.1(0.34;0.16)	2.12(0.34;0.16)
C(N ₁)	2.11(0.31;0.15)	2.09(0.31;0.15)	2.11(0.31;0.15)	2.12(0.31;0.15)	2.1(0.31;0.15)	2.1 (0.31;0.15)	2.11(0.31;0.15)
V(C _{sp} ³ , C _{sp} ²)	2.15(1.06;0.5)	2.16(1.07;0.5)	2.14(1.06;0.49)	2.14(1.06;0.5)	2.16(1.07;0.49)	2.14(1.06;0.49)	2.14(1.06;0.5)
V(C,O ₁)	2.16(1.25;0.58)	2.22(1.27;0.57)	2.26(1.28;0.57)	2.22(1.27;0.57)	2.14(1.24;0.58)	2.27(1.28;0.57)	2.22(1.27;0.57)
V(C,N ₁)	2.96(1.43;0.48)	2.79(1.39;0.5)	2.65(1.34;0.51)	2.19(1.15;0.52)	2.18(1.15;0.53)	2.13(1.12;0.53)	2.86(1.41;0.49)
V(H,N ₁)	1.99(0.79;0.4)	2.0(0.79;0.4)	1.99(0.8;0.4)	1.99(0.78;0.39)		1.97(0.77;0.39)	2.0(0.79;0.4)
V ₁ (O ₁)	2.74(1.22;0.45)	2.78(1.24;0.45)	2.77(1.22;0.44)	2.73(1.22;0.45)	2.75(1.23;0.45)	2.74(1.23;0.45)	2.72(1.22;0.45)
V ₂ (O ₁)	2.8(1.24; 0.44)	2.7(1.22;0.45)	2.68(1.21;0.45)	2.76(1.23; 0.45)	2.79(1.24;0.45)	2.7 (1.2; 0.44)	2.75(1.23;0.45)
V ₁ (N ₁)	1.04(0.73;0.7)	1.24(0.81;0.66)	1.37(0.86;0.63)	0.78(0.59;0.76)	0.92(0.67;0.73)	0.99 (0.69;0.7)	1.14(0.77;0.68)
V ₂ (N ₁)	-	-	-	1.03(0.72;0.7)	1.07(0.74;0.7)	0.78(0.58;0.75)	-
V(N ₁ , C)	1.7(0.96;0.56)	1.69(0.96;0.57)	1.67(0.96;0.57)	1.69(0.95;0.57)	1.67(0.95;0.57)	-	1.72(0.97;0.56)
V ₁ (O ₁)U V ₁ (O ₁)	5.54e	5.48e	5.45e	5.49e	5.54e	5.44e	5.47e
V ₁ (N ₁)U V ₁ (N ₁)	1.04e	1.24e	1.37e	1.81e	1.99e	1.77e	1.14e

exchange between these basins and the vicinal bonding domains (intramolecular interaction) .

The relationship of change between the electron density on the O and X atoms and the values of bond order in this region, we can describe these bonds by the resonance structures $C(=O) - X \leftrightarrow O^- - C = X^+$ highlighting the fact that the electronegativity of O is larger than N and that the latter can accommodate a positive charge more easily, a much smaller contribution of the ionic mesomeric limit structure ($O^- - C = X^+$) in esters is expected.

In general terms, the inductive effects in the C(=O)-X backbone as the general trend that points that the stabilization by resonance will be larger when at the acyl group are linked to less electronegative alkyl groups. Thus, the resonant effect will be important in structures with $-C_2H_4-NH_2$ and $-C_2H_5$ moieties and less important in structures with electron-withdrawal substituents [$-CH(CH_3)(C_6H_5)$; $-CH(C_6H_5)_2$; $-CH_2(C_6H_5)$].

On the other hand, taking into account the small contribution of a resonance structure with a formal positive

charge on the highly electronegative O atom, the amides present greater stabilization by resonance than the esters and their stabilization decreases with the deviation from planarity of the C(=O)–X skeleton. In this context, as τ increases its value (Tables 4 and 5) there is less charge transfer from the N₁ and O₂ atoms to the acyl oxygen in the Ispd and Vpa. The double bond character of the carbonyl group C=O increases slightly (notice that this effect is more important in amide than esters) and the character of double bond of C–N and C–O linkages decreases. In all the compounds the change of the N–C and O–C bonds (population and bond order) with the τ -twist value seems to be minor.

When we consider the general trend of the inductive effects in C(=O)–X there seems no clear correlation between the expected reorganization of electron density in the basins V(C,O₁) and V(C,N₁) and the electron-releasing effect of the alkyl substituents. For instance, comparing the topological properties of C=O and C–N bonds between the Etpvd-Dmvp and Etpvd-Ipvpd structures, it is interesting to notice the significant loss of electrons in the basin V(C,O₁) of Dmvpd in contrast with the value predicted for V(C,N₁) and the important increment of the population of basin V(C,N₁) in Ipvpd regarding the electron depopulation expected due to the decreasing of the planarity in the C(=O)N.

For the change of the non-bonding electron density of O and N atoms related to structural data it is possible to note some trends along the series such that a less electronegative R_{1,2} induces a larger concentration of the electron density in basins V_{1,2}(O₁), V_{1,2}(N₁), V_{1,2}(O₂) and the population of these basins changes inversely with the twisting around the C–X bond, the topological properties of these domains do not show a clear relationship with the increase of τ .

We believe that the important difference observed on the electronic distribution V_{1,2}(O₁), V_{1,2}(X_{1,2}), V(C,O) and V(C,N) along the series of compounds may be explained by considering not only the shift in the lability of the nitrogen lone pair (pyramidalization N) and the accepting power of the CO group due to structural modification of C(=O)–X but also due to the existence of secondary interactions donor-acceptor type among the non-bonding electron pairs and vicinal V(H,C) domains which play a dominant role in maintaining of a planar conformation of C(=O)–X.

To elucidate these features we investigate the delocalization of the electron density in the C(=O)–X moiety and adjacent basins by decomposition of the basin fluctuation (σ^2) into covariance contribution cov[Ω_i , Ω_j]. Each value in Table 5 represents the correlation between the basin population calculated for the domains V_{1,2}(O₁), V_{1,2}(X_{1,2}), V(C,O₁), V(C,X_{1,2}), V(H, X_{1,2}), V(X_{1,2},C) and vicinal V(H,C) domains (Fig. 6) *i.e.*, V_{1,2}(O₁) ↔ V(C,O₁) = (1), V_{1,2}(O₁) ↔ V(C,X_{1,2}) = (2), V(C,O₁) ↔ V(C,X_{1,2}) = (3), V(C,

X_{1,2}) ↔ V(X_{1,2},C) = (4), (Fig. 6-a); V(C,X_{1,2}) ↔ V_{1,2}(X_{1,2}) = (5), V(X_{1,2},C) ↔ V_{1,2}(X_{1,2}) = (6), V(H,X_{1,2}) ↔ V_{1,2}(X_{1,2}) = (7), (Fig. 6-b); V(C,X_{1,2}) ↔ V_{1,2}(H,X_{1,2}) = (8), V(H,X_{1,2}) ↔ V(X_{1,2},C) = (9), V(H,C) ↔ V_{1,2}(O₁) = (10), V(H,C) ↔ V_{1,2}(X_{1,2}) = (11), V(C,C) ↔ V(H,C) = (12), V(X_{1,2},C) ↔ V(H,C) = (13), V(X_{1,2},C) ↔ V(C,C) = (14) (Fig. 6-c); V(H, X₁)/V(X₂) ↔ V(H, C_a) = (15), V(H, X₁)/V(X₂) ↔ V(H, C) = (16), V(H, C_a) ↔ V(H, C_a) = (17) (Fig. 6-d).

The contribution of V_{1,2}(O₁) to the delocalization in V(C,O₁) and V(C,X_{1,2}) found to be almost constant in all the series of compounds, going from amides to esters and Vpa: cov[V(C,O₁), V_{1,2}(O₁)] = (1) show an increase from 0.75 to 0.81e while cov[V(C,X_{1,2}), V_{1,2}(O₁)] = (2) and cov[V(C,O₁), V(C,X_{1,2})] = (3) decrease from 0.09 to 0.05e and from 0.14 to 0.10e, respectively (Table 6). Regarding the values of (4) and (5), while in the esters the contribution of V(X_{1,2},C) and V_{1,2}(X_{1,2}) to the C–X_{1,2} bond is almost constant; in amides there are slight changes.

Examining the change in the V(C,X_{1,2}), V_{1,2}(X_{1,2}) V(H, X₁) and V(X_{1,2},C) basins due to exchange (4), (5), (6), and (7) one can derive quite useful information about the trends in electron distribution within this molecule. Thus, we can remark that:

- i) σ delocalization is not an important effect in the stabilization of planar C(=O)–X group [since (3) does not change with respect to (4) and (5) shifts],
- ii) the exchange between the electron densities of the C–X_{1,2} and X_{1,2}–C bonds [(4)] may not be envisioned as a flow charge that evidence the lost of double bond character of C–X_{1,2} bonds and the changes do not show a clear correlation with the electronegativity of substituents,
- iii) in amides the (5) delocalization increases with the decrease of electronegativity of the group linked to N amidic, while this exchange remains almost unchanged in the esters,
- iv) while the electronic delocalization in the X_{1,2}–C and H–X_{1,2} bonds [(6) and (7)] increase as the pyramidalization of X_{1,2} (χ_N , χ_{O2}) do, a change without showing an order that regulate the exchange value along the series of derivatives can be observed on the value of contributions of the adjacent basins to the V(H,X_{1,2}) link [(8) and (9)].

Important exceptions to the trend described above can be noticed by considering the value of contribution (5), (6), and (7) determined for Bzvpd and Ipvpd. In these structures the picture offered by our covariance contribution may be interpreted examining the information on the electron density contribution of O₁ and X_{1,2} at the vicinal V(H,C) basins [(10) and (11)].

The decomposition of the basin fluctuation (σ^2) into covariance contributions reveal an interpenetration of the

Table 5 Basins populations (N), the population variance σ^2 (N) and relative fluctuation λ in propyl valproate (Prvpa), isopentyl valproate (Isvpa), 1-secbutanol valproate (Secbvpa), benzyl valproate (Benzvpa) and valproic acid (Vpa)

	<i>Prvpa</i>	<i>Isovpa</i>	<i>Secvpa</i>	<i>Benvpa</i>	<i>Vpa</i>
Basins. Ω	$N_{\Omega} (\sigma^2; \lambda)$	$N_{\Omega} (\sigma^2; \lambda)$	$N_{\Omega} (\sigma^2; \lambda)$	$N_{\Omega} (\sigma^2; \lambda)$	$N_{\Omega} (\sigma^2; \lambda)$
Properties R=(Pr)₂ = -CH₂ CH₂-CH₃					
C(C)	2.09(0.26;0.13)	2.09(0.26;0.13)	2.09(0.26;0.13)	2.09(0.26;0.13)	2.09(0.26;0.13)
V(C,C)	1.86(0.99;0.53)	1.86(0.99;0.53)	1.86(0.99;0.53)	1.86(0.99;0.53)	1.86(0.99;0.53)
V(H,C)	2.01(0.66;0.33)	2.0(0.66;0.33)	2.0(0.66;0.33)	2.01(0.66;0.33)	2.01(0.66;0.33)
Properties R₁= alkyl					
C(C)	2.09(0.26;0.13)	2.09(0.26;0.13)	2.09(0.26;0.13)	2.08(0.27;0.13)	-
V(C,C)	1.87(0.98;0.53)	1.89(0.99;0.53)	1.92(1.0;0.52)	-	-
V(H,C)	2.02(0.65;0.32)	2.01(0.66;0.33)	2.02(0.66;0.33)	2.07(0.66;0.32)	-
C(O ₃)	-	-	2.12 (0.35;0.16)	-	-
V(C;O ₃)	-	-	1.41(0.89;0.63)	-	-
V(H,O ₃)	-	-	1.74(0.83;0.47)	-	-
V ₁ (O ₃)	-	-	2.26(1.09;0.48)	-	-
V ₂ (O ₃)	-	-	2.32(1.10; 0.48)	-	-
Properties R₁= aryl					
C(C _i)	2.09(0.26;0.13)	2.09(0.26;0.13)	2.09(0.26;0.13)	2.08(0.27;0.13)	-
V(C _{sp} ³ , C _{sp} ³)	-	-	-	2.09(1.05;0.5)	-
V(C _{sp} ³ , C _{sp} ²)	-	-	-	2.77(1.31;0.47)	-
V(C _{sp} ² , C _{sp} ²)	-	-	-	2.77(1.31;0.47)	-
V(H, C _{sp} ³)	-	-	-	2.15(0.67;0.31)	-
V(H, C _{sp} ²)	-	-	-	2.15(0.67;0.31)	-
Properties C(=O)-O					
C(C)	2.10(0.26;0.12)	2.08(0.26;0.12)	2.09(0.26;0.12)	2.08(0.26;0.12)	2.09(0.25;0.12)
C(O ₁)	2.11(0.35;0.17)	2.1(0.35;0.15)	2.11(0.34;0.16)	2.09(0.35;0.17)	2.12(0.34;0.16)
C(O ₂)	2.10(0.35;0.17)	2.12(0.34;0.16)	2.12(0.35;0.16)	2.12(0.37;0.17)	2.11(0.34;0.16)
V(C,C)	2.19(1.07;0.49)	2.18(1.07;0.49)	2.19(1.07;0.49)	2.2(1.08;0.49)	2.18(1.07;0.49)
V(C,O ₁)	2.4(1.34;0.56)	2.41(1.34;0.56)	2.34(1.31;0.56)	2.4(1.34;0.56)	2.45(1.35;0.55)
V(C,O ₂)	1.71(1.01;0.59)	1.7(1.01;0.59)	1.72(1.02;0.59)	1.67(1.0;0.6)	1.61(0.97;0.55)
V ₁ (O ₁)	2.67(1.22;0.46)	2.67(1.21;0.45)	2.77(1.23;0.45)	2.67(1.22;0.46)	2.69(1.20;0.45)
V ₂ (O ₁)	2.67(1.2;0.45)	2.67(1.2;0.45)	2.62(1.21; 0.46)	2.7(1.22;0.45)	2.61(1.18; 0.45)
V(O ₂ , C ₉)	1.39(0.87;0.62)	1.41(0.88;0.62)	1.44(0.89;0.62)	1.39(0.87;0.63)	-
V(H,O ₂)	-	-	-	-	1.79(0.82;0.46)
Properties R₂= Lone electron pairs O₂					
V ₁ (O ₂)	4.45(1.54;0.35)	4.43(1.54;0.35)	1.74(1.55;0.35)	4.46(1.56;0.35)	2.21(1.10; 0.50)
V ₂ (O ₂)	-	-	4.41(1.55;0.35)	-	2.15(1.08; 0.50)
V ₁ (O ₁)U V ₁ (O ₁)	5.34e	5.34e	5.39e	5.37e	5.30e
V ₁ (O ₂)U V ₁ (O ₂)			6.15e		4.36e

V_{1,2}(O₁) , V_{1,2}(X_{1,2}) into V(H,C) basins in the vicinity of the plane C(=O₁)-X_{1,2}. (Table 6).

The contribution of V_{1,2}(O₁) and V_{1,2}(X_{1,2}) to the total delocalization of V(H,C) described by the number of exchanged electrons in (10) and (11) increase with the τ value from 0.06 to 0.16e and from 0.02 to 0.16e respectively (percentage contribution to σ^2 of the protonated basins ~10% to 23%). Regarding the electrons delocal-

ization between the V(H,X₁) and V(X₂) basins and the adjacent V(H,C) basins [(15–17)] while the contribution (15) is constant in all the series of compounds and a slightly larger effect of correlation for the exchange (16) in the Etavpd, Isvpa, and Secvpa was found only for Dmvpd it has observed that the electrons in V(H, C α) are correlated with adjacent C–H functional groups (0.04e; percentage contribution ~6%).

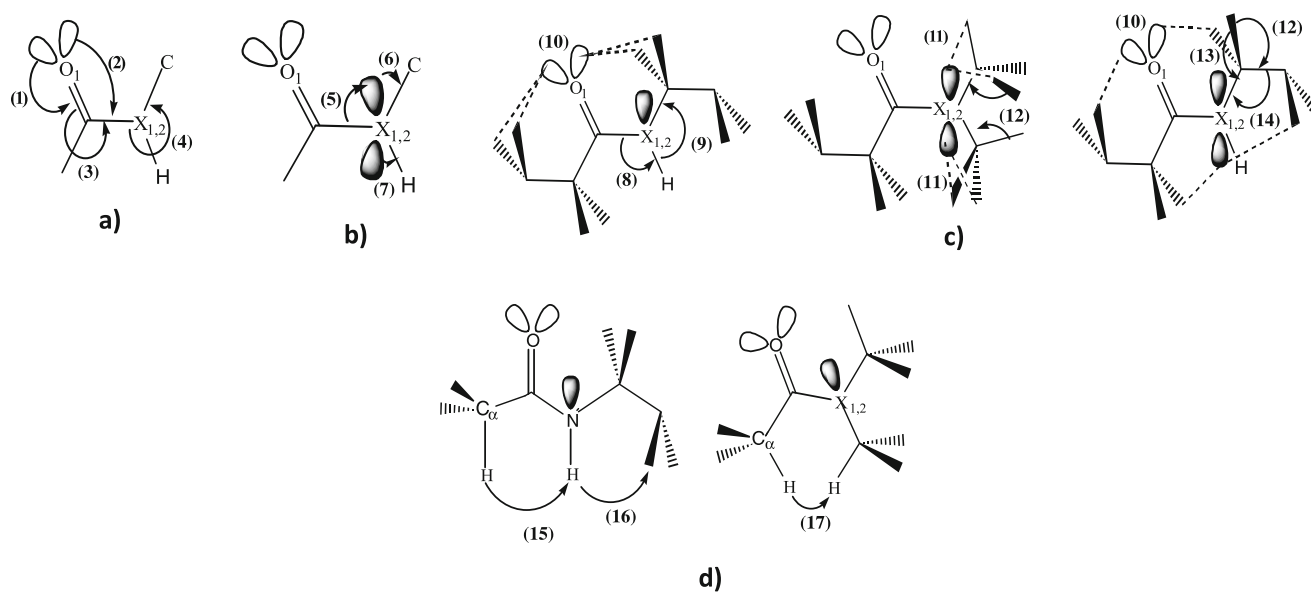


Fig. 6 Schematic representation of a exchange contribution in $C(=O)-X_{1,2}$ **(a)** electronic delocalization between the domains $V_{1,2}(O_1) \leftrightarrow V(C,O_1) = (1)$, $V_{1,2}(O_1) \leftrightarrow V(C,X_{1,2}) = (2)$, $V(C,O_1) \leftrightarrow V(C,X_{1,2}) = (3)$, $V(C,X_{1,2}) \leftrightarrow V(X_{1,2},C) = (4)$, $V(C,X_{1,2}) \leftrightarrow V_{1,2}(X_{1,2}) = (5)$, $V(X_{1,2},C) \leftrightarrow V_{1,2}(X_{1,2}) = (6)$, $V(H,X_{1,2}) \leftrightarrow V_{1,2}(X_{1,2}) = (7)$, **(b)** electronic correlations between the basins $V(C,X_{1,2}) \leftrightarrow V_{1,2}(H,X_{1,2}) =$

(8) , $V(H,X_{1,2}) \leftrightarrow V(X_{1,2},C) = (9)$, $V(H,C) \leftrightarrow V_{1,2}(O_1) = (10)$, $V(H,C) \leftrightarrow V_{1,2}(X_{1,2}) = (11)$, $V(C,C) \leftrightarrow V(H,C) = (12)$, and **(c)** exchange contribution between the domains $V(X_{1,2},C) \leftrightarrow V(H,C) = (13)$, $V(X_{1,2},C) \leftrightarrow V(C,C) = (14)$, $V(H,X_1)/V(X_2) \leftrightarrow V(H,C_\alpha) = (15)$, $V(H,X_1)/V(X_2) \leftrightarrow V(H,C)_{rest} = (16)$, $V(H,C_\alpha) \leftrightarrow V(H,C) = (17)$.

The picture offered by the contributions **(10–17)** (Table 6) reveals the existence of not only non-conventional intramolecular hydrogen bond patterns such as $C-H \dots O/N$, but also of an inherently weaker closed-shell stabilizing interaction of the type dihydrogen bonding $C-H \dots H-N/C$. The $H \dots H$ distances are significantly shorter than twice the van der Waals radius of a hydrogen atom, $\sim 2.4 \text{ \AA}$ (range $d_{H \dots H} = 1.826\text{--}2.237 \text{ \AA}$) where there is no net electrical charges on the hydrogen atoms ($C_\alpha - H \dots H - C$) or, due to the difference of electronegativity of acceptor (N) and donor (C) units of hydrogen bonding, there is a small difference of charges of the same sign between the H atoms [31–34].

The predicted intramolecular interaction confirm a belt of hydrogen bonds around $C(=O)-X$ moiety connecting the four, five or six-member ring defined by the predicted hydrogen bridges (Fig. 7). The stabilization caused by these interactions were measured by an increasing of the contribution **(10–11)** and **(15–17)** fall with the enhanced donor-acceptor separation (Table 6, Fig. 7). Our results also indicate that the neighbor hydrogen-bond interactions will be significant at distances comparable to those described in the Dmvpd (Table 6). This structure presents a symmetric and flexible structural environment that allows the formation of a hydrogen bridge closing large ring (five or six-member ring, see Fig. 7). Here hydrogen bonded atoms are connected through a conjugated framework which facilitates a charge flow from hydrogen to the oxygen atom,

enhancing the hydrogen bridge strength and offsetting the bending strain that causes the closure of the ring. We found that **(12)**, **(13)**, and **(14)** (Table 6) entail a rather complex electronic redistribution resulting of simultaneous interactions strongly influenced by factors such as the degree of polarization of π -system in the $C(=O)-X$, the electronegativity of the connected N-acyl, pyramidalization of C and $X_{1,2}$ and the establishment of stabilizing electronic interaction between of unshared electron of O_1 , $X_{1,2}$ and geminal and vicinal bonds (Fig. 7, hyperconjugation).

Comparing the change of the values of **(12–14)** with the contributions **(4–7)**, we note that as increasing contribution of the electronic exchange increases in **(10–11)** and **(15–17)**, a flow of electrons is established counteracting the increase in the polarities of the bonds due to the formation of hydrogen bonds (enhance electronic exchange **(12–14)** and decrease **(3)** and **(1)**].

Similarly, can be seen an additional polarization in the amide group [increase **(4–5)**, **(7–8)** and **(13)**] by π -bond contribution [31–34] due to the lability of the nitrogen lone pair to correlate with adjacent flexible hydrogen-bonding functional groups (C-H) in the vicinity of N acceptor that leads us directly to the concept of resonance assisted hydrogen bonding (RAHB) [31–34]. In this context and as our calculation shows clearly, strong hydrogen bonding increasing the double-bond character and hence the torsional rigidity of $C-X_{1,2}$ bond are possible when the polarizable system of π -bonds in $C(=O)-X$ is surrounded

Table 6 Cross contribution to the population variance in C(=O)₁-X_{1,2} skeleton of amides and esters of Vpa and mean C-O₁/X_{1,2} (Å) and H-O₁/X_{1,2} separations (Å) for intramolecular C-H...O/X_{1,2} and C-H... H-X₁/H-C hydrogen bonds

Order	Cov[Ω _i , Ω _j]	Amides					Esters						
		Etavpd	Aphvpd	Bzvpd	Etvpd	Dmvpd	Vpd	Ipvpd	Prvpa	Isvpa	Secvpa	Benvpa	Vpa
(1)	cov[V(C,O ₁),V _{1,2} (O ₁)]	0.75	0.77	0.77	0.77	0.74	0.78	0.76	0.80	0.81	0.79	0.81	0.81
(2)	cov[V(C,N),V _{1,2} (O ₁)]	0.09	0.07	0.09	0.07	0.07	0.07	0.09	0.05	0.05	0.05	0.05	0.05
(3)	cov[V(C,O ₁),V(C,X _{1,2})]	0.14	0.13	0.13	0.13	0.13	0.12	0.14	0.11	0.11	0.11	0.11	0.10
(4)	cov[V(C,X _{1,2}),V(X _{1,2} ,C)]	0.22	0.11	0.20	0.11	0.21	-	0.22	0.10	0.10	0.10	0.10	-
(5)	cov[V(C,X _{1,2}),V _{1,2} (X _{1,2})]	0.23	0.33	0.25	0.33	0.36	0.36	0.24	0.49	0.49	0.49	0.49	0.46
(6)	cov[V(X _{1,2} ,C),V _{1,2} (X _{1,2})]	0.14	0.24	0.15	0.11	0.26	-	0.37	0.41	0.41	0.41	0.40	0.27
(7)	cov[V(H,X ₁),V _{1,2} (X _{1,2})]	0.17	0.31	0.20	0.31	-	0.31	0.18	-	-	-	-	0.54
(8)	cov[V(C,X _{1,2}),V(H,X ₁)]	0.29	0.15	0.26	0.15	-	0.17	0.28	-	-	-	-	-
(9)	cov[V(H,X ₁),V(X _{1,2} ,C)]	0.13	0.12	0.13	0.13	-	0.17	0.13	0.80	-	-	0.81	-
(10)	cov[V(H,C),V _{1,2} (O ₁)]	0.06	0.06	0.08	0.06	0.08	0.03	0.08	0.05	0.07	0.07	0.16	0.03
(11)	cov[V(H,C),V _{1,2} (X _{1,2})]	0.02	0.04	0.04	0.07	0.16	-	0.03	0.13	0.12	0.11	0.11	0.27
(12)	cov[V _{1,2} (C,C),V(H,C)]	0.15	0.18	0.23	0.15	-	-	0.16	0.16	0.16	0.18	0.19	-
(13)	cov[V(X _{1,2} ,C),V(H,C)]	0.24	0.14	0.12	0.25	0.36	-	0.17	0.19	0.17	0.10	0.17	-
(14)	cov[V(X _{1,2} ,C),V(C,C)]	0.09	0.21	0.22	0.09	-	-	0.18	0.07	0.07	0.07	0.07	-
(15)	cov[V(H,X ₁)/V(O ₂),V(H,C _α)]	0.02	0.02	0.02	0.02	-	0.02	0.02	0.02	0.02	-	-	-
(16)	cov[V(H,X ₁)/V(O ₂),V(H,C) _{rest}]	0.04	0.01	0.03	0.03	-	-	0.02	0.03	0.12	0.09	0.11	-
(17)	cov[V(H,C _α),V(H,C) _{rest}]	-	-	-	-	0.04	-	-	-	-	-	-	-
Mean donor-acceptor separations for C-H-O/X_{1,2} and C-H... H-X_{1,2}/H-C hydrogen bonds													
C-H...O	C-O ₁ (Å)	2.86	2.82	2.69	2.83	2.85	2.95	2.90	2.67	2.77	2.54	2.56	2.25
	H-O ₁ (Å)	2.42	2.52	2.46	2.42	2.48	2.65	2.56	2.62	2.61	2.34	2.48	2.26
C-H...X _{1,2}	C-X _{1,2} (Å)	2.55	2.50	2.56	2.50	2.58	2.51	2.39	2.38	2.38	2.69	1.45	2.94
	H-X ₁ /H-C(Å)	2.75	2.85	2.84	2.78	-	-	2.74	2.40	2.40	2.66	2.90	2.94
CH...HX ₁ /C	H-H-X ₁ /H-C(Å)	2.13	2.17	2.17	2.16	1.83	2.23	2.18	2.08	2.08	2.06	2.02	2.66
		2.58	2.76	2.48	2.85	-	-	2.52	2.38	2.42	2.52	2.65	2.67

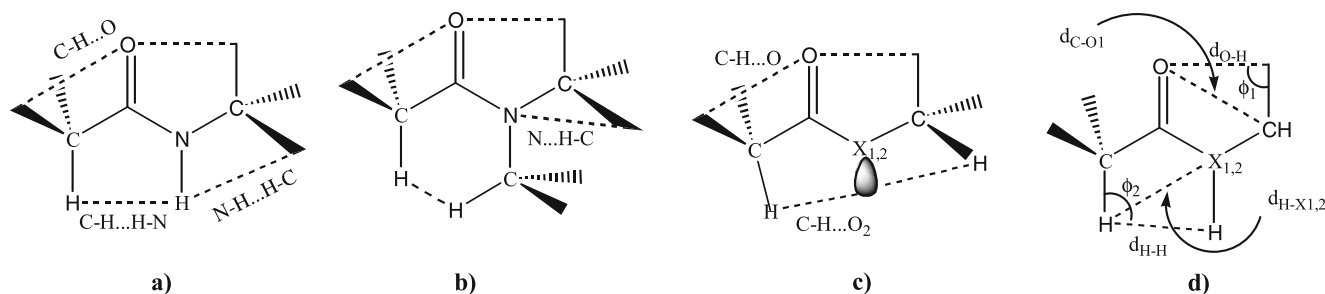


Fig. 7 Schematic view of hydrogen bonds belt around $C(=O)-X$ forming by $C-H...O/N$ and $C-H...H-X_1/O_2$ interaction in (a) amide moiety with an asymmetrical structural environment: belt connecting four and five-membered ring, (b) amide moiety with a symmetrical structural

environment: belt of hydrogen bonds connecting four, five and six-membered ring, (c) belt of hydrogen bonds in esters. (d) Definition of the structural parameters $d_{C...O_1}$, $d_{H...X_{1,2}}$, $d_{O_1...H}$, $d_{H...H}$, $\phi_1 = \angle C-H...O$ and $\phi_2 = \angle C-H...X_{1,2}$

itself by a symmetric electronic and flexible structural environment which allows the charge flow through covalent bonds from the donor to the acceptor hydrogen bonding.

As a final consideration that reinforces the interpretation of the covariance analysis, it is worth mentioning that while the magnitude of electron transfer between valence localization domains participating in the H-bonds and the range of observed hydrogen-bond lengths in our structures are in line with the criterion formulated [31–34] as the basins involved in the intramolecular interactions undergo important contraction in its volume with respect to determined volume of $C-H$ vicinal basins that are not involved in hydrogen bonds (Table 7). This has been interpreted by Pacios [31–34] who remarks that upon hydrogen bonding, ELF domains associated to H-donor and H-acceptor groups

exert a mutual pressure due to the Pauli repulsion between electron pairs that flattens the localization domains.

In effect, such as described by Pacios [31–34], while the volume of ELF basins $V(O_1)$, $V(X_{1,2})$ and $V(H, C)$, $V(H, X_1)$ involved in the H-bond decreases dramatically, the volume of the $V(O_1)$, $V(X_{1,2})$ and $V(H, C)$ basins involved in the H-bond remains nearly constant and they are higher. Results in Table 7 indicate also that the H-acceptor of O_1 , $X_{1,2}$ ability increases as the charge associated to its lone pairs increases and the H-donor ability of $H-X_1$ must increase as the charge associated to $V(H, X_1)$ decrease.

Turning to the main topic of this paper, bearing in mind the results reported in [12, 13] the relative potency ($ED_{50}V_{PA}/ED_{50}drugs$) to suppress seizures induced in the test MES follows the order $Etvpd [6] > Dmvpd \sim Vpd [2.9] > Ipvpd \sim Prvpa [2.6] > Vpa [1.7]$ and considering the

Table 7 Volume (Vol) and populations (N_Ω) of ELF basins of the $V(O_1)$, $V(X_{1,2})$ and $V(H, C)$, $V(H, X_1)$ basins. **A**) Volume (Vol) and populations (N_Ω) of basins involved in the H-bond, and **B**) Volume (Vol) and populations (N_Ω) of basins not involved in the H-bond

Compounds	A					B		
	Vol- N_Ω $V_2(O_1)$	Vol- N_Ω $V_1(X_{1,2})$	Vol- N_Ω $V(H-C_\alpha)$	Vol- N_Ω $V(H.X_1)$	Vol- N_Ω $V(H.C)_{rest}$	Vol- N_Ω $V_1(O_1)$	Vol- N_Ω $V_2(X_{1,2})$	Vol- N_Ω $V(H.C)_{rest}$
Etavpd	58.89 - 2.80	21.31 - 1.04	62.97 - 2.04	63.19 - 1.99	62.28 - 2.04	62.7 - 2.74	-	75.81 - 2.00
Aphvpd	58.70 - 2.77	17.83 - 0.80	63.14 - 2.04	48.58 - 1.99	56.80 - 2.05	57.09 - 2.72	21.33 - 1.02	74.87 - 2.03
Bzvpd	57.54 - 2.75	24.59 - 1.31	56.68 - 2.04	49.48 - 2.00	52.17 - 2.03	55.94 - 2.68	-	78.64 - 2.03
Etvpd	58.34 - 2.76	16.39 - 0.78	63.25 - 2.03	54.38 - 1.99	65.17 - 2.04	60.72 - 2.73	23.83 - 1.03	76.23 - 2.00
Dmvpd	56.96 - 2.79	17.89 - 0.92	54.73 - 2.04	-	62.55 - 2.02	60.77 - 2.75	21.24 - 1.07	74.20 - 2.00
Vpd	70.14 - 2.69	29.66 - 0.85	62.51 - 2.04	59.28 - 1.97	-	58.47 - 2.75	33.24 - 0.94	74.65 - 2.01
Ipvpd	57.71 - 2.75	23.82 - 1.14	58.28 - 2.04	50.08 - 2.00	-	58.42 - 2.72	-	75.86 - 2.00
Prvpa	56.21 - 2.68	62.54 - 4.42	57.49 - 2.04	-	66.83 - 2.07	58.22 - 2.67	-	76.00 - 2.00
Ispvpa	54.89 - 2.67	66.60 - 4.43	61.47 - 2.03	-	61.66 - 2.07	58.73 - 2.67	-	74.75 - 2.01
Secvpa	48.02 - 2.62	59.98 - 4.42	62.60 - 2.03	-	62.38 - 2.16	65.63 - 2.75	-	76.13 - 2.00
Benvpa	48.48 - 2.64	65.80 - 4.47	62.27 - 2.03	-	64.55 - 2.08	63.41 - 2.71	-	77.13 - 2.04
Vpa	63.20 - 2.69	42.03 - 2.15	62.24 - 2.02	-	-	67.41 - 2.61	42.67 - 2.21	74.95 - 2.01

ligand-receptor complementarities during the process of molecular recognition drug-receptor, our data allows us highlight structural requirements complementary to those reported in [12, 14] on selectivity by antiepileptics activity.

In fact, while relatively strong intramolecular interaction as those described in the Vpa, Prvpa, and Dmvpd seem not to meet the specificity requirements that are necessary for the involved biological process, an important electronic and structural arrangement as that described for Etpvd, which helps the accumulation of charge on the proton donor/acceptor units maximizing its hydrogen bonding donor/acceptor capabilities putting both entities in the coplanar form appears to be an important requirement. Likewise, a electronic reorganization where the hyperconjugative interactions are weak [(11)] and $X_{1,2}$ is capable to undergo changes on its hybridization and polarization leading to decrease of its hydrogen bonding acceptor capabilities as is predicted for Ipvpd, Vpd, Bzvpd, Aphvpd, and Etavpd appears to be a rather strong limitation that would seriously impede the flow of biological information during the process of molecular recognition drug-receptor.

Based on our considerations, new ideas emerge to take into account in the development of new antiepileptic that are related with the caution and handling of the vectorial properties and sensibility to stereochemistry of the hydrogen bonds.

Conclusions

We have examined some structural and electronic properties of Vpa and derivatives which posses anticonvulsant activity, by using the topological analysis of ELF. The results show a $Y-C(=O)-XR_1R_2$ [where $R=CH_3-(CH_2)_2-$; $X=N,O$ and $R_1, R_2=H$; alkyl and aryl rest and lone pair electrons (lp)] molecular fragment with complex electronic and structural features that we interpreted using as descriptor the decomposition of the basin fluctuation (σ^2) into covariance contributions $cov[\Omega_i, \Omega_j]$.

A systematic study of the bonds in $C(=O)-X_{1,2}$ reveals an electronic organization resulting from simultaneous interaction strongly influenced by several factors. These factors are: a) the degree of polarization of π -system in the $C(=O)-X_{1,2}$, b) the electronegativity of the connected N-acyl, c) the position of $X_{1,2}$ electron lone pair with respect to the π -system, d) pyramidalization of C and $X_{1,2}$, and e) the establishment of stabilizing electrostatic interaction between of unshared electron in $O_1/X_{1,2}$ and geminal and vicinal C–H bonds (non-conventional hydrogen bond).

On the basis of these features, it is suggested that the biological activity of the compounds is conditioned by the degree and directionality of the resonance induced by the belt of intramolecular hydrogen bonds connecting hydrogen

bridge closing four, five or six-member ring offset the repulsive interaction and bending strain that cause mainly remarkable out-of plane bending occurs around the $C-X_{1,2}$.

Acknowledgments N.C.C. acknowledges a fellowship from the Consejo Nacional de Investigaciones Científicas y Tecnológicas (CONICET) and financial support from Dr Patricio Fuentealba to visit his lab. A.H.J., is a member of the Research Scientific Career (CIC-PBA), E.A.C is a member of the Research Scientific Career CONICET.

References

- White HS (2003) Preclinical development of antiepileptic drugs: past, present, and future directions. *Epilepsia* 44(suppl 7):2–8
- Keane PE, Simiand J, Mendes E, Santucci V (1983) The effects of analogues of valproic acid on seizures induced by pentylenetetrazol and GABA content in brain of mice. *Neuropharmacol* 22:875–879
- Loscher W, Nau H (1985) Pharmacological evaluation of various metabolites and analogues of valproic acid. Anticonvulsant and toxic potencies in mice. *Neuropharmacol* 24:427–435
- Lindhout D, Meinardi H (1984) Spina bifida and in-utero exposure to valproic acid. *Lancet* II:396
- Jager-Roman E, Deichl A, Jakob S, Hartmann A, Koch S, Rating D, Steldinger R, Nau H, Helge H (1986) Fetal growth, major malformations, and minor anomalies in infants born to women receiving valproic acid. *J Pediatr* 108:997–1004
- Nau H, Loscher W (1986) Pharmacologic evaluation of various metabolites and analogs of valproic acid teratogenic potencies in mice. *Fundam Appl Toxicol* 6:669–676
- Bialer M, Hadad S, Kadry B, Abdul-Hai A, Haj-Yehia A, Sterling J, Herzig Y, Yagen B (1996) Pharmacokinetic analysis and antiepileptic activity of tetra-methylcyclopropane analogues of valpromide. *Pharm Res* 13:284–289
- Bialer M (1991) Clinical pharmacology of valpromide. *Clin Pharmacokinet* 20:114–122
- Haj-Yehia A, Bialer M (1989) Structure-pharmacokinetic relationships in a series of valpromide derivatives with antiepileptic activity. *Pharm Res* 6:682–689
- Haj-Yehia A, Hadad S, Bialer M (1992) Pharmacokinetic analysis of the structural requirements for forming “stable” analogues of valpromide. *Pharm Res* 9:1058–1063
- Spiegelstein O, Kroetz DL, Levy RH, Yagen B, Hurst SI, Levi M, Haj-Yehia A, Bialer M (2000) Structure activity relationship of human microsomal epoxide hydrolase inhibition by amide and acid analogues of valproic acid. *Pharm Res* 17:216–221
- Tasso S, Bruno-Blanch L, Estiú G (2001) Design, synthesis, and anticonvulsant activity of some sulfamides. *J Mol Model* 7:231–239
- Tasso S, Moon S, Bruno-Blanch L, Estiú G (2004) Characterization of the anticonvulsant profile of valpromide derivatives. *Bioorg. Med Chem* 12:3857–3869
- Gavernet L, Dominguez Cabrera MJ, Bruno-Blanch L, Estiú G (2007) Design, synthesis, and anticonvulsant activity of some sulfamides. *Bioorg Med Chem* 15:5604–5614
- HyperChem Release 7.5 for Windows. Hypercube, USA, 2002
- Peng C, Ayala PY, Schlegel HB, Frisch MJ (1996) Using redundant internal coordinates to optimize equilibrium geometries and transition states. *J Comp Chem* 17:49–56
- Gaussian 03, Revision B.04. Gaussian, Pittsburgh, 2003
- Becke A (1993) Density-functional thermochemistry. III. The role of exact exchange. *J Chem Phys* 98:5648–5652

19. Lee C, Yang W, Parr R (1988) Development of the Colle-Salvetti correlation-energy formula into a functional of the electron density. *Phys Rev B* 37:785–789
20. Nour S, Krokidis XF, Fuster B, Silvi (1997) TopMod Package, Paris
21. Noury S, Krokidis X, Fuster F, Silvi B (1999) Computational Tools for the Electron Localization Function Topological Analysis. *Computers and Chemistry* 23:597–604
22. Flükiger P, Lüthi HP, Portmann S, Weber J (2000) MOLEKEL 4.0. Swiss Center for Scientific Computing, Manno
23. Savin A (2005) The electron localization function (ELF) and its relatives: interpretations and difficulties. *J Mol Struct* 727:127–131
24. Becke AD, Edgecombe KE (1990) A simple measure of electron localization in atomic and molecular systems. *J Chem Phys* 92:5397–5403
25. Silvi B, Savin A (1994) Classification of Chemical bonds based on topological analysis of electron localization functions. *Nature* 371:683–686
26. Savin A, Silvi S, Colonna F (1996) Topological analysis of the electron localization function applied to delocalized bonds. *Can J Chem* 74:1088–1096
27. Gillespie RJ, Hargittai I (1991) *The VSEPR Model of Molecular Geometry*. Allyn & Bacon, Boston
28. Allen FH, Kennard O, Watson DG, Brammer L, Orpen AG, Taylor R (1987) Tables of bond lengths determined by X-Ray and neutron diffraction. Part 1. Bond lengths in organic compounds. *J Chem Soc Perkin Trans II*:S1–S19
29. Dunitz JD (1995) X-Ray analysis of the structure of Organic Molecules. Verlag Helvetica Chimica Acta, CH-4010 Basel, Switzerland
30. Berski S, Gajewski G, Latajka Z (2007) Electron localization function (ELF) study on intramolecular delocalization of the electron density in the H₂X, H₂C=X and XO₂ (X = O, S, Se, Te) molecules: Role of the atomic core and lone pair. *J Mol Struct* 844–845:278–285
31. Bakhmutov V (2008) *Dihydrogen bond: Principles, Experiments, and Applications*. Wiley-Interscience, New Jersey
32. Grabowski SJ (2006) *Hydrogen Bonding - New Insights*. Springer, The Netherlands
33. Gilli G, Bellucci F, Ferreti V, Gilli P (1989) Evidence for resonance-assisted hydrogen bonding from crystal-structure correlations on the enol form of the beta-diketone fragment. *J Am Chem Soc* 111:1023–1028
34. Alikhani M, Fuster F, Silvi B (2005) What can tell the topological analysis of ELF on hydrogen bonding? *Struct Chem* 16:203–210